

Analysis of The Vehicle Routing Problem Solved via Hybrid Quantum Algorithms in Presence of Noisy Channels

1stNishikanta Mohanty, *Centre for Quantum Software and Information, University of Technology Sydney, Ultimo, Sydney 2007, NSW, Australia*
Nishikanta.M.Mohanty@student.uts.edu.au

2nd Bikash K. Behera, *Bikash's Quantum (OPC) Pvt. Ltd., Mohanpur 741246, WB, India*
bikas.riki@gmail.com

3rd Christopher Ferrie, *Centre for Quantum Software and Information, University of Technology Sydney, Ultimo, Sydney 2007, NSW, Australia*
Christopher.Ferrie@uts.edu.au

Abstract—The Vehicle routing problem (VRP) is an NP-hard optimization problem that has been an interest of research for decades in science and industry. The objective is to plan routes of vehicles to deliver goods to a fixed number of customers with optimal efficiency. Classical tools and methods provide good approximations to reach the optimal global solution. Quantum computing and quantum machine learning provide a new approach to solving combinatorial optimization of problems faster due to inherent speedups of quantum effects. Many solutions of VRP are offered across different quantum computing platforms using hybrid algorithms such as quantum approximate optimization algorithm and quadratic unconstrained binary optimization. In this work, we build a basic VRP solver for 3 and 4 cities using the variational quantum eigensolver on a fixed ansatz. The work is further extended to evaluate the robustness of the solution in several examples of noisy quantum channels. We find that the performance of the quantum algorithm depends heavily on what noise model is used. In general, noise is detrimental, but not equally so among different noise sources.

Index Terms— Ising Model, Combinatorial Optimization, Variational Quantum Eigensolver, Quantum Noise Channels
Ising Model, Combinatorial Optimization, Variational Quantum Eigensolver, Quantum Noise Channels

I. INTRODUCTION

Quantum computing is a generation of computing technology that is expected to solve complex optimization problems at a considerable speedup compared to classical counterparts. One of the key benefits of quantum computing is its parallelism [1], [2] which has been proposed as a mechanism to speed up computations for complex optimization scenarios (quantum approximate optimization algorithm (QAOA) [3], adiabatic computation (AC) [4], Grover's algorithm [5], and others) to quickly compute the global optimum. Classical optimization algorithms in machine learning (ML) often take a significant amount of time to compute when applied to a multidimensional problem and require considerable CPU and GPU resources [6]. In general, it has been observed that classical algorithms perform inefficiently when dealing with higher dimensional problem space [7]. This is in large part

due to the fact that ML algorithms are tasked with solving optimization problems that are NP-hard in their complexity [6].

The vehicle routing problem (VRP) is one such combinatorial optimization problem. As per an industry perspective, VRP comes under the category of routing problems that try to address multiple issues related to fleet management [8]. The objective is always to optimize vehicle movement such that it minimizes the cost or maximizes the profit. VRP is a computationally difficult problem for which many exact and heuristic algorithms have been proposed, but providing fast and reliable solutions is challenging [8], [9]. Describing the VRP in its simplest form, a single vehicle is tasked to deliver goods at multiple customer locations; also, the vehicle must return to pick up additional items when it runs out of goods [10]. The objective is to optimize an available set of routes, all starting and ending at a given node, called the depot, to attain the maximum possible reward, which is often the negative of the total distance traveled or average service time. This problem is computationally difficult to solve optimally, even with only a few hundred customer nodes, and is classified as an NP-hard problem [6].

Any VRP (n, k) involves $(n - 1)$ locations with k vehicles and a depot D [11], [8]. Its solution is the set of routes where all k vehicles begin and end at the specified depot D , so that each location is visited once. The lowest total distance covered by k vehicles constitutes the optimal route. This problem can be referred to as a generalization of the classical traveling salesman problem [12], [9], where now a group of k salesmen has to serve collectively $(n - 1)$ locations, such that each location is served exactly once [8]. In most real-world applications, the VRP problem is generally augmented by constraints, such as vehicle capacity or limited coverage time. Thus, many classical and quantum solutions have been proposed to arrive at a solution efficiently. Current quantum approaches for solving optimization problems include QAOA [11], QUBO [13], [14], quantum annealing [15], [16], [17], and VQE [11], which we will define in detail later.

In this work, we study this classic problem in a different light. Here we explore adding controlled noise to an adapted quantum solution to determine if it improves or degrades the overall results. In this context, we came across recent works in QAOA [18], [19], [20], [21] and VQE algorithms [22], which look at the generic effects of noise in these hybrid algorithms. Our work complements these results by analysing the effects of noise in a detailed gate-based simulation of an algorithm to solve VRP. We analyze the effect of various noise channels on an existing, yet variable, ansatz that is developed as a solution to VRP. We apply amplitude damping, bit-flip, phase-flip, bit-phase-flip and depolarising noise channels to VRP circuits and analyze the effects and consolidate our findings.

The paper is organized as follows. Sec. II discusses the fundamental mathematical concepts such as combinatorial optimization, adiabatic computation, QAOA, and the Ising model. Sec. III discusses the formulation of VRP using the concepts discussed in previous Section. Sec. IV covers the basic building blocks of circuits to solve VRP. Sec. V covers the building of ansatz for VRP. Finally, Sec. VI covers the effects of applying noise models on the VRP circuit. In Sec. VII, we conclude by comparing the effects of various noise models on the VRP circuit and future directions of research.

II. MATHEMATICAL BACKGROUND

The fundamental concepts of solving routing problems rest in dealing with techniques and procedures to solve combinatorial optimization problems. This is followed by converting the mathematical models to a quantum equivalent mathematical model for formulating the objective function. The solution of the objective function is often achieved by maximization or minimization of the function. In this section, we outline the key concepts.

A. Combinatorial Optimization

A classical combinatorial optimization (CO) problem is the task of finding an optimal object from a finite set of objects. Exhaustive search is not practical in finding the optimal object due to the potentially high number of objects. CO problems are maximization or minimization problems with input strings in some set S and m clauses with $|S|$ greater than equal to m . Each clause takes as input a string and returns a value. The total cost function of a string is the sum over the m clauses. If we denote the input string as z and clauses as C_α then the total cost function is written as,

$$C(z) = \sum_{\alpha=1}^m C_\alpha(z). \quad (1)$$

The goal is to find $\bar{z} \in S$ such that $C(\bar{z}) \geq C_\alpha(z)$ for all $z \in S$ (in the case of minimization, $C(\bar{z}) \leq C_\alpha(z)$ for all $z \in S$). Here \bar{z} need not be unique. For simplification, restrictions are put on clauses and input strings where clauses are restricted to integers 0 and 1, whereas input strings are restricted to a binary representation of integers 0 through $2^n - 1$. Hence z can be written as $z = z_0 z_1 z_2 \dots z_{n-1}$ for

$z_i \in \{0, 1\}$. Also, considering only maximization problems, the minimization problems can be studied as $C'_\alpha(z) = 1 - C_\alpha(z)$

$$\begin{aligned} C'(z) &= \sum_{k=0}^{m-1} C'_\alpha(z) = \sum_{k=0}^{m-1} (1 - C_\alpha(z)), \\ &= m - \sum_{k=0}^{m-1} C_\alpha(z) = m - C(z). \end{aligned} \quad (2)$$

B. Adiabatic Quantum Computation

Adiabatic quantum computation (AQC) is a theoretical framework of a quantum computer [4], [23]. The principle behind AQC is the adiabatic theorem, which states that if a Hamiltonian is altered slowly enough, a system in the ground state of that Hamiltonian will remain in the ground state [24]. The Hamiltonian represents the energy state of a system. In AQC, we deal with two Hamiltonians: the driver Hamiltonian (H_d) and the problem Hamiltonian (H_p). The driver Hamiltonian (H_d) is a ground state of a system that is easy to prepare, whereas the problem Hamiltonian (H_p) is the desired state we are interested, and is obtained as a ground state after evolution [4]. The time required is determined by the minimal energy difference between the interpolating Hamiltonian's two lowest states.

In general, we are unable to assess this disparity. In other words, we begin with an easy-to-prepare ground state (i.e., the ground state of (H_d)) and hope to end up with the quantum state we want (i.e., the ground state of (H_p)), which is usually significantly challenging to prepare. Mathematically, we have a function $s(t)$ on $[0, T]$ where $s(0) = 0$ and $s(T) = 1$. T is the value of time set high enough for the adiabatic theorem to hold. We define the Hamiltonian, $H(t) = (1 - s(t))H_D + s(t)H_P$. By the adiabatic theorem, given an appropriate $s(t)$, we stay in the ground state of this $H(t)$ during the entire interval $[0, T]$. Therefore, we can see that at time $t = 0$, we are in the ground state of (H_d) and by time $t = T$, we are in the desired ground state of (H_p). The time evolution under this time-dependent Hamiltonian involves an integral that is hard to evaluate:

$$U(t) = \tau \exp \left\{ \frac{-i}{\hbar} \int_0^t H(T) dT \right\}. \quad (3)$$

Trotterization technique [25] can be used to evaluate this Hamiltonian. We discretize $U(T)$ into intervals of δt small enough that the Hamiltonian is approximately constant over each interval. This allows us to use the much cleaner formula for the time-independent Hamiltonian. If $U(b, a)$ represents time evolution from time a to time b ,

$$\begin{aligned} U(T, 0) &= U(T, T - \delta t) U(T - \delta t, T - 2\delta t) \dots U(\delta t, 0), \\ &= \prod_{j=1}^p U(j\delta t, (j-1)\delta t), \\ &\approx \prod_{j=1}^p e^{-iH(j\delta t)\delta t}. \end{aligned} \quad (4)$$

Where the approximation improves as p gets larger (or, equivalently, as δt gets smaller) and we have chosen δt to be in units of \hbar . Now using the approximation $e^{i(A+B)x} = e^{iAx}e^{iBx} + \mathcal{O}(x^2)$ and adding Hamiltonian $H(j\delta t) = (1-s(j\delta t))H_D + s(j\delta t)H_P$ the integral $U(t)$ becomes,

$$U(T, 0) \approx \prod_{j=1}^p e^{-i(1-s(j\delta t))H_D\delta t} e^{-is(j\delta t)H_P\delta t}. \quad (5)$$

This AQC can be approximated by letting the system evolve under H_P for some small $s(j\delta t)\delta t$ and then H_D for some small $(1-s(j\delta t))\delta t$ and unitaries can be constructed for these operations $U = e^{-i\alpha H\delta t}$, Where α is some number in the interval $[0, 1]$, and that incorporates the scaling due to $s(j\delta t)$. AQC forms the theoretical basis of variational quantum algorithm QAOA, which is discussed briefly in ongoing section.

C. QAOA

Quantum Approximate Optimization Algorithm (QAOA) is a variational algorithm proposed by Farhi *et al.* in 2014 [4], [3]. This algorithm relies on the framework of adiabatic quantum computation. It is an algorithm that uses both classical and quantum techniques thus, it is a hybrid algorithm. In the previous section, we touch upon the quantum adiabatic computation where we move from the eigenstate of driver Hamiltonian to that of the eigenstate of problem Hamiltonian. The problem Hamiltonian can be written as,

$$C|z\rangle = \sum_{\alpha=1}^m C_{\alpha(z)}|z\rangle. \quad (6)$$

We know that the maximum energy eigenstate of C is the solution to the combinatorial optimization problem. Similarly, for driver Hamiltonian we use

$$B = \sum_{j=1}^n \sigma_j^x. \quad (7)$$

where σ_j^x is the σ^x Pauli operator on bit z_j also know as the mixing operator. Let us also define $U_c(\gamma) = e^{-i\gamma C}$ and $U_B(\beta) = e^{-i\beta B}$ which lets the system evolve under C for some γ amount of time and under B for some β amount of time, respectively. Basically, QAOA constructs a state

$$|\beta, \gamma\rangle = e^{-i\beta_p B} e^{-i\gamma_p C} \dots e^{-i\beta_2 B} e^{-i\gamma_2 C} e^{-i\beta_1 B} e^{-i\gamma_1 C} |s\rangle, \quad (8)$$

where $|s\rangle$ is a superposition state of all input qubits. The expectation value of the cost function $\sum_{\alpha=1}^m \langle \beta, \gamma | C | \beta, \gamma \rangle$ gives the solution or the approximate solution of the problem [26].

D. Ising Model

The Ising model is a classic mathematical model for ferromagnetism in statistical mechanics [27], [28]. The model is made up of discrete variables that represent magnetic dipole moments of atomic ‘‘spins’’ in one of two states (+1 or -1). The spins are arranged in a graph, typically a lattice (in which the local structure repeats periodically in all directions), which allows each spin to interact with its neighbors. Neighboring spins that agree have less energy than those that disagree; the system tends to the lowest energy, but heat disrupts this tendency, allowing alternative structural phases to emerge. As a simplified model of reality, the model enables for the identification of phase transitions [29]. The total energy of the spins is described by the following Hamiltonian

$$H_c = - \sum_{\langle i,j \rangle} J_{ij} \sigma_i \sigma_j - h \sum \sigma_i. \quad (9)$$

Where J_{ij} represents the interaction between i and j , which are adjacent spins, and h represents an external magnetic field. If J is positive, the ground state at $h = 0$ is a ferromagnet. If J is negative, the ground state at $h = 0$ is an anti-ferromagnet for a bipartite lattice. Hence for simplification and in the context of this document, we can write the Hamiltonian as

$$H_c = - \sum_{\langle i,j \rangle} J_{ij} \sigma_i^z \sigma_j^z - \sum h_i \sigma_i^x. \quad (10)$$

Here σ_z and σ_x represent Pauli z and x operator. For simplification, we can consider the following conditions, $J_{ij} = \pm 1$ to ferromagnetic ($J_{ij} > 0$), $h = 0$ assuming no external influence on spin. Thus we can rewrite the Hamiltonian as following

$$H_c = - \sum_{\langle i,j \rangle} J_{ij} \sigma_i^z \sigma_j^z = - \sum_{\langle i,j \rangle} \sigma_i^z \sigma_j^z. \quad (11)$$

E. VQE

The Variational Quantum Eigensolver (VQE) is another hybrid quantum classical algorithm that is used to estimate the eigenvalue of a large matrix or Hamiltonian H [30]. The basic objective of this method is to search for a trial qubit state of a wave function $|\psi(\vec{\theta})\rangle$ which is dependent on a parameter set $\vec{\theta} = \theta_1, \theta_2, \dots$ also called as the variational parameters. By quantum theory the expectation of an observable or Hamiltonian H in a state $|\psi(\vec{\theta})\rangle$ can be expressed as,

$$E(\vec{\theta}) = \langle \psi(\vec{\theta}) | H | \psi(\vec{\theta}) \rangle. \quad (12)$$

By spectral decomposition

$$H = \lambda_1 |\psi\rangle_1 \langle \psi|_1 + \lambda_2 |\psi\rangle_2 \langle \psi|_2 + \dots + \lambda_n |\psi\rangle_n \langle \psi|_n. \quad (13)$$

Where λ_i and $|\psi\rangle_i$ are the eigenvalues of matrix H . Also the eigenstates of H are orthogonal so $\langle \psi_i | \psi_j \rangle = 0$ if $i \neq j$. The wave function $|\psi(\vec{\theta})\rangle$ can be expressed as superposition of eigenstates

$$|\psi(\vec{\theta})\rangle = \alpha_1(\vec{\theta})|\psi\rangle_1 + \alpha_2(\vec{\theta})|\psi\rangle_2 + \dots + \alpha_n(\vec{\theta})|\psi\rangle_n. \quad (14)$$

Thus the expectation becomes

$$E(\vec{\theta}) = |\alpha_1(\vec{\theta})|^2\lambda_1 + |\alpha_2(\vec{\theta})|^2\lambda_2 + \dots + |\alpha_n(\vec{\theta})|^2\lambda_n. \quad (15)$$

Clearly, $E(\vec{\theta}) \geq \lambda_{\min}$. So in VQE algorithm, we vary the parameters $\vec{\theta} = \theta_1, \theta_2, \dots$ until $E(\vec{\theta})$ is minimized. This property of VQE is useful in solving combinatorial optimization problems where a parameterized circuit is used to prepare the trial state of the algorithm, and $E(\vec{\theta})$ is called as the cost function that is the expectation value of the Hamiltonian in the trial state. Iterative minimization of the cost function produces the ground state of the target Hamiltonian. The optimization process utilizes a classical optimizer which uses quantum computer to evaluate the cost function and calculate its gradient at each optimization step.

III. MODELLING VRP IN QUANTUM

To find a solution to the vehicle routing problem, we can map the cost function to an Ising Hamiltonian H_c [29]. The minimization of Ising Hamiltonian H_c gives the solution to the problem. To begin, let us consider an arbitrary connected graph of n vertices and $n - 1$ edges. Also, let us assume we have to route a vehicle among two vertices of the graph which are not adjacent. To formulate this, let us consider a binary decision variable x_{ij} who has a value 1 if there exists an edge between i and j for edge weight $w_{ij} > 0$ else, the value is 0. Now to represent VRP problem, we need $n \times (n - 1)$ decision variables. For every edge from $i \rightarrow j$ we define two sets of nodes $source[i]$ and $target[j]$. The set $source[i]$ contains the nodes j to which i sends an edge $j \in source[i]$. The set $target[j]$ contains the nodes i to which i sends an edge $i \in target[j]$. We define VRP as follows,

$$VRP(n, k) = \min_{\{x_{ij}\}_{i \rightarrow j \in \{0,1\}}} \sum_{i \rightarrow j} w_{ij}x_{ij}. \quad (16)$$

Where k is the number of vehicles and n is total number of locations, but considering the starting location as 0^{th} location or Depot D we have $n - 1$ locations for vehicles to travel. This is of course subject to the following constraints,

$$\begin{aligned} \sum_{j \in source[i]} x_{ij} &= 1, \forall i \in \{1, \dots, n-1\}, \\ \sum_{j \in target[i]} x_{ji} &= 1, \forall i \in \{1, \dots, n-1\}, \\ \sum_{j \in source[0]} x_{0j} &= k, \\ \sum_{j \in target[0]} x_{j0} &= k. \end{aligned} \quad (17)$$

From the above set of constraints, the first two impose the restriction that each node must be visited only once by the delivering vehicle. The last two constraints enforce the restriction that the vehicle must return to the depot after

delivering the goods. For the VRP equation and constraints, we can form the Hamiltonian of VRP as follows [11].

$$\begin{aligned} H_{VRP} &= H_A + H_B + H_C + H_D + H_E, \\ H_A &= \sum_{i \rightarrow j} w_{ij}x_{ij}, \\ H_B &= A \sum_{i \in \{1, \dots, n-1\}} \left(1 - \sum_{j \in source[i]} x_{ij} \right)^2, \\ H_C &= A \sum_{i \in \{1, \dots, n-1\}} \left(1 - \sum_{j \in target[i]} x_{ji} \right)^2, \\ H_D &= A \left(k - \sum_{j \in source[0]} x_{0j} \right)^2, \\ H_E &= A \left(k - \sum_{j \in target[0]} x_{j0} \right)^2. \end{aligned} \quad (18)$$

$A > 0$ is a constant. The set of all binary decision variables x_{ij} can be represented in vector form as

$$\vec{x} = [x_{(0,1)}, x_{(0,2)}, \dots, x_{(1,0)}, x_{(1,2)}, \dots, x_{(n-1, n-2)}]^T. \quad (19)$$

Using the above vector, we can define two additional vectors for each node (in the beginning of the section we defined two sets for source and target nodes so two vectors will represent) $\vec{z}_{S[i]}$ and $\vec{z}_{T[i]}$.

$$\begin{aligned} \vec{z}_{S[i]} &= \{x_{ij} = 1, x_{kj} = 0, k \neq i, \forall j, k \in \{0, \dots, n-1\}\}, \\ \vec{z}_{T[i]} &= \{x_{ji} = 1, x_{jk} = 0, k \neq i, \forall j, k \in \{0, \dots, n-1\}\}. \end{aligned} \quad (20)$$

The above vectors will assist in the formulation of the QUBO model of VRP. In general, the QUBO model [31], [13], [14], [32] of a connected graph $G = (N, V)$ is defined as,

$$f(x)_{QUBO} = \min_{x \in \{0,1\}^{(N \times V)}} x^T Q x + g^T x + c. \quad (21)$$

where, Q is a quadratic coefficient of the edge weights, g is a linear coefficient of the node weights and c is a constant. Here, \mathbb{J} is the matrix of all ones, \mathbb{I} is the identity matrix, and $e_0 = [1, 0, \dots, 0]^T$. Hence for QUBO formulation of Eq. (18) the coefficients are given as follows,

$$\begin{aligned} Q &= A \left[[z_{T[0]}, \dots, z_{T[n-1]}]^T [z_{T[0]}, \dots, z_{T[n-1]}] \right. \\ &\quad \left. + (\mathbb{I}_n \otimes \mathbb{J}(n-1, n-1)) \right], \\ g &= W - 2Ak \left((e_0 \otimes \mathbb{J}_{n-1}) + [z_{T[0]}]^T \right), \\ &\quad + 2A(\mathbb{J}_n \otimes \mathbb{J}_{n-1}), \\ c &= 2A(n-1) + 2Ak^2. \end{aligned} \quad (22)$$

The binary decision variable x_{ij} is transformed to spin variable $s_{ij} \in \{-1, 1\}$ as $x_{ij} = (s_{ij} + 1)/2$.

From the above Eqs, we can expand the Eq. (21) to form the Ising Hamiltonian of VRP [13]

$$H_{Ising} = - \sum_i \sum_{i < j} J_{ij} s_i s_j - \sum_i h_i s_i + d. \quad (23)$$

Here, the terms J_{ij} , h_i and d are defined as follows,

$$\begin{aligned} J_{ij} &= -\frac{Q_{ij}}{2}, \quad \forall i < j, \\ h_i &= \frac{g_i}{2} + \sum_j \frac{Q_{ij}}{4} + \sum_j \frac{Q_{ji}}{4}, \\ d &= c + \sum_i \frac{g_i}{2} + \sum_i \sum_j \frac{Q_{ij}}{4}. \end{aligned} \quad (24)$$

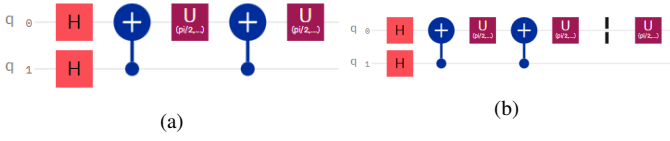


Fig. 1: (a) Sample circuit showing gate selections for H_{cost} . (b) Sample circuit showing gate selections with additional u gate for H_{mixer} .

IV. ANALYSIS AND CIRCUIT BUILDING

In this section, we create a gate-based circuit to realize the above formulation using the IBM gate model, which we have implemented using the Qiskit framework [33]. For any arbitrary VRP problem using qubits, we begin with the state of $|+\rangle^{\otimes n(n-1)}$ the ground state of H_{mixer} by applying the Hadamard to all qubits initialized as zero state, and we prepare the following state.

$$|\beta, \gamma\rangle = e^{-iH_{mixer}\beta} e^{-iH_{cost}\gamma} \dots e^{-iH_{mixer}\beta_0} e^{-iH_{cost}\gamma_0} |+\rangle^{n \otimes (n-1)}. \quad (25)$$

The energy E of the state $|\beta, \gamma\rangle$ is calculated by expectation of H_{cost} from Eq. (12). Again From the Ising model, H_{cost} term can be written in terms of Pauli operators as,

$$H_{cost} = - \sum_i \sum_{i < j} J_{ij} \sigma_i^z \sigma_j^z - \sum_i h_i \sigma_i^z - d. \quad (26)$$

Thus for a single term of state in $|\beta, \gamma\rangle$ as β_0, γ_0 , the expression reads, $e^{-iH_{mixer}\beta_0} e^{-iH_{cost}\gamma_0}$. The first term H_{cost} can be expanded to following,

$$\begin{aligned} e^{iJ_{ij}\gamma_0\sigma_i\sigma_j} &= \cos J_{ij}\gamma_0 I + i \sin J_{ij}\gamma_0 \sigma_i \sigma_j, \\ &= \begin{bmatrix} e^{iJ_{ij}\gamma_0} & 0 & 0 & 0 \\ 0 & e^{-iJ_{ij}\gamma_0} & 0 & 0 \\ 0 & 0 & e^{-iJ_{ij}\gamma_0} & 0 \\ 0 & 0 & 0 & e^{iJ_{ij}\gamma_0} \end{bmatrix} \\ &= M \end{aligned} \quad (27)$$

Applying $CNOT$ gate on before and after the above matrix 'M' we can swap the diagonal elements,

$$CNOT(M)CNOT = \begin{bmatrix} e^{iJ_{ij}\gamma_0} & 0 & 0 & 0 \\ 0 & e^{-iJ_{ij}\gamma_0} & 0 & 0 \\ 0 & 0 & e^{iJ_{ij}\gamma_0} & 0 \\ 0 & 0 & 0 & e^{-iJ_{ij}\gamma_0} \end{bmatrix}. \quad (28)$$

Observing the upper and lower blocks of matrix we can rewrite,

$$\begin{bmatrix} 1 & 0 \\ 0 & 1 \end{bmatrix} \otimes \begin{bmatrix} e^{iJ_{ij}\gamma_0} & 0 \\ 0 & e^{-iJ_{ij}\gamma_0} \end{bmatrix} = I \otimes e^{iJ_{ij}\gamma_0} \begin{bmatrix} 1 & 0 \\ 0 & e^{-2iJ_{ij}\gamma_0} \end{bmatrix}. \quad (29)$$

$\begin{bmatrix} 1 & 0 \\ 0 & e^{-2iJ_{ij}\gamma_0} \end{bmatrix}$ is a phase gate. Looking at the 2nd term of H_{cost} we get,

$$\begin{aligned} H_{cost} &= \sum_i h_i \sigma_i^z, \\ e^{ih_i\sigma_i} &= \cos h_i\gamma_0 I + i \sin h_i\gamma_0 \sigma_i, \\ &= \cos h_i\gamma_0 \begin{bmatrix} 1 & 0 \\ 0 & 1 \end{bmatrix} + i \sin h_i\gamma_0 \begin{bmatrix} 1 & 0 \\ 0 & -1 \end{bmatrix}, \\ &= \begin{bmatrix} e^{ih_i\gamma_0} & 0 \\ 0 & e^{-ih_i\gamma_0} \end{bmatrix}. \end{aligned} \quad (30)$$

Fig. 1a depicts the basic circuit with two qubits along with gate selections for H_{cost} . Similarly H_{mixer} is just a rotation along X axis denoted by a U gate depicted in Fig. 1b.

V. VQE SIMULATION OF VRP

We construct the VRP circuit using the above equations and create the Hamiltonians for 3 city and 4 city scenarios. Since we need $n(n-1)$ qubits we end up Hamiltonians and circuits with 6 and 12 qubits only. Beyond 4 cities, it is not possible to simulate in a classical desktop computer due to memory limitations. We create the ansatz using a complete set of random weights between 0 and 1 and run it across various VQE optimizers available in IBM Qiskit framework namely COBYLA, L_BFGS_B, SPSA, and SLSQP. We run the circuit up to 4 layers across all the optimizers and obtain the results depicted in Fig. 2. It is clear that COBYLA is the best performing optimizer followed by SPSA, L_BFGS_B and finally SLSQP. However, in the following, when we pass the circuit through various noise models, we will use only the COBYLA and the L_BFGS_B optimizer.

VI. NOISE MODEL SIMULATION OF VQE

In quantum noisy environment, a pure input state will be transformed into a mixed state represented as a density matrix [20], [34]. Considering a 6-qubit state, $|\psi\rangle_{q_0 q_1 q_2 q_3 q_4 q_5}$ is a pure state with a density matrix defined as $\rho =$

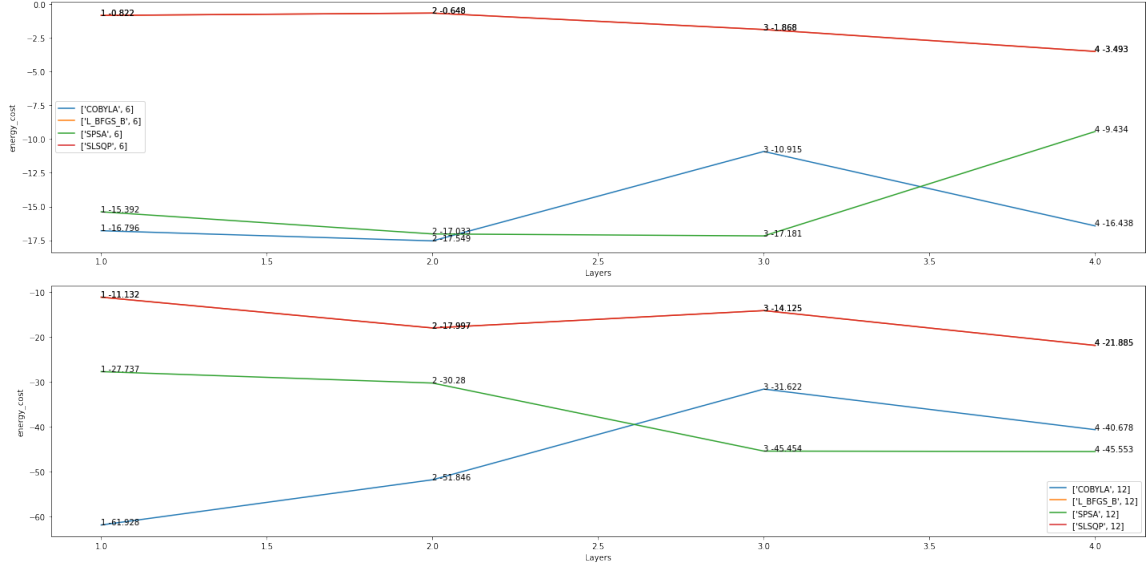


Fig. 2: Plot illustrating the circuit simulation of VRP with 5 layers using various optimizers (COBYLA, L_BFGS_B, SLSQP, SPSA). The plot consists of two separate graphs depicting simulation output of 6 qubit and 12 qubit circuits respectively. Each plot in turn consists of four lines indicating energy values for separate optimizers. The minimum value at each Layer is represented in pairs with (layer, minimum energy) format.

$|\psi\rangle_{q_0 q_1 q_2 q_3 q_4 q_5}$. After the implementation of the noise model, the density matrix takes the following form,

$$\xi_r(\rho) = \sum_m (E_m^{rq^0})(E_m^{rq^1}) \dots (E_m^{rq^5}) \rho \times (E_m^{xq^0})^\dagger (E_m^{xq^1})^\dagger \dots (E_m^{xq^5})^\dagger, \quad (31)$$

where $r \in \{A, B, W, F, D\}$. The elements of the noise channels are described as follows, A is amplitude damping noise, B is bit-flip noise, W is phase-flip noise, F is bit-phase-flip noise, and D is depolarising noise. In our case, we apply these noise channels to our VRP circuit and ansatz which is variable based on the number of qubits (6 or 12) and layers (1 to 5). For simulation purpose, we choose the optimizer COBYLA as its has the best performance characteristics in simulation of VQE. We restrict the noise probability to 0.5 as noisy environments beyond this level of noise is unlikely and irrelevant in practice. In following subsections we discuss the noise channels and operators we experimented on in the VRP circuit.

A. Amplitude Damping

The energy dissipation is a consequence of interaction of quantum system with an amplitude damping channel. In simple terms, a quantum system gaining or losing energy from or to its environment is described as change in its amplitude or amplitude damping [34], [35]. If κ_A is the probability of gain or loss of amplitude or decoherence rate; the Kraus operators of amplitude damping channel can be described as follows (Eq. (32)),

$$E_0^A = \begin{bmatrix} 1 & 0 \\ 0 & \sqrt{1 - \kappa_A} \end{bmatrix}, \quad E_1^A = \sqrt{\kappa_A} \begin{bmatrix} 0 & 1 \\ 0 & 0 \end{bmatrix}. \quad (32)$$

B. Bitflip Noise

Bitflip noise is characterised by random bit-flip errors [35] with probability $0\kappa_B$. Thus, the Kraus operators of bit-flip noise channel can be described as Eq. (33),

$$E_0^B = \sqrt{1 - \kappa_B} I, \quad E_1^B = \sqrt{\kappa_B} X = \sqrt{\kappa_B} \begin{bmatrix} 0 & 1 \\ 1 & 0 \end{bmatrix}. \quad (33)$$

C. Phase Flip Noise

Phase-flip noise alters the phase parameter of quantum system without exchange of energy [34], [35]. The decoherence rate or the phase-flip noise parameter also follows the simple Bernoulli distribution with probability parameter κ_W , thus the Kraus operators of phase-flip noise channel can be defined as Eq. (34),

$$E_0^W = \sqrt{1 - \kappa_W} I, \quad E_1^W = \sqrt{\kappa_W} Z = \sqrt{\kappa_W} \begin{bmatrix} 1 & 0 \\ 0 & -1 \end{bmatrix}. \quad (34)$$

D. Bit-Phase Flip Noise

Bit-phase flip noise channel is characterised by combination of random bit-flip errors along with change in phase information of the quantum system without loss of energy [35]. Similar to other noise channels, the decoherence rate or the combined probability of bit-phase flip error follows the distribution κ_F . The Kraus operator of the bit-phase flip channel could be given by Eq. (35),

$$E_0^F = \sqrt{1 - \kappa_F} I, \quad E_1^F = \sqrt{\kappa_F} Y = \sqrt{\kappa_F} \begin{bmatrix} 0 & -i \\ i & 0 \end{bmatrix}. \quad (35)$$



Fig. 3: Plot illustrating the average EnergyCost of VRP with 4 layers using various NoiseModels (Amplitude damping , Bit-flip, Bit-phase-flip, Phase-flip, and Depolarising noise). The plot consists of two separate charts depicting simulation output of 6 qubit and 12 qubit circuits respectively. The minimum value at each Layer is represented in pairs with (layer, minimum energy) format.

E. Depolarizing Noise

A depolarizing noise channel is one that either leaves the system untouched or replaces it with a maximally mixed state of I/d for a d -level quantum system. The decoherence rate or the depolarization noise probability follows the distribution with parameter κ_D . The Kraus operators as follows,

$$\begin{aligned}
 E_0^D &= \sqrt{1 - \kappa_D} I, \\
 E_1^D &= \sqrt{\frac{\kappa_D}{3}} X = \sqrt{\frac{\kappa_D}{3}} \begin{bmatrix} 0 & 1 \\ 1 & 0 \end{bmatrix}, \\
 E_2^D &= \sqrt{\frac{\kappa_D}{3}} Y = \sqrt{\frac{\kappa_D}{3}} \begin{bmatrix} 0 & -i \\ i & 0 \end{bmatrix}, \\
 E_3^D &= \sqrt{\frac{\kappa_D}{3}} Z = \sqrt{\frac{\kappa_D}{3}} \begin{bmatrix} 1 & 0 \\ 0 & -1 \end{bmatrix}.
 \end{aligned} \tag{36}$$

It is to be noted that, in all the cases, the noise channel is applied locally to each circuit.

VII. INFERENCES FROM SIMULATION

In the experiment of simulating VRP across various noise channels we vary the noise probability from 0.05 to 0.5 and observe the energy values of VQE. We execute the VRP circuit with 1 to 4 layers with our chosen optimizer COBYLA for both 6 qubit and 12 qubit configurations. The experiment is repeated 10 times for each noise model with different noise realizations. In the same experiment, we calculate the minimum eigenvalue of classical Hamiltonian and record the difference of energy cost after induction of noise. The energy of the state is recorded for each layer of the QAOA circuit from 1 to 4. These values are averaged over the 10 iterations to arrive at the average energy cost for each value of noise parameter and each layer number. The results are depicted in Fig. 3 and summarized in Table I. The deviation from the optimal value is shown in Table II.

We note that VQE values are impacted due to the induction of noise channels. Amplitude damping noise shows values range between 50% to 75% of classical minimum for both 6 qubit (-17.68) and 12 qubit (-65.684) circuits. There are a few outliers wherein some parameter values of high noise, the algorithm is able to reach very close to the classical minimum for 6 qubit circuits. For 12 qubit circuits, the values are mostly above 50% of classical minimum but never reaches as close as in 6 qubit circuits. However this trend is seen across multiple layers for amplitude damping channel. In plots, we see the global minimum across layers is observed at 2nd layer at -48.947 but it is very close to the minimum of 1st layer at -47.219 . Hence we can infer that for amplitude damping channel, increasing the layers dose not necessarily improve the results.

For the bit-flip noise channel, we note that the the VQE values are 50% or above of the classical minimum for the first layer but it degrades to around 25% for 2nd layer, falling further on 3rd and finally close to zero on 4th. Since this trend is seen in both 6 qubit and 12 qubit circuits, we can infer that for bit-flip noise channel, increasing the number of layers only degrades the VQE values.

There is a similar story for the bit-phase-flip channel. The VQE values are 25% percent or above of the classical minimum for the first layer but they degrades as the layers increase for 6 qubit. For 12 qubit circuits, the VQE values are consistently poor.

Finally, for both depolarising and phase-flip channels, the VQE values remain close to zero for both 6 qubit and 12 qubit circuits. It appears that bit-phase-flip, depolarising, and phase-flip noise channels are the most detrimental in VQE circuits.

In addition to the may hours of testing and debugging, it is to be noted that the results reported here amounted to 219 hours of CPU time on a standard laptop computer using Qiskit's built-in simulators [33].

VIII. DISCUSSION AND CONCLUSION

In this work, we studied the effects of noise in a gate-based simulation of an algorithm to solve the vehicle routing problem. We applied amplitude damping, bit-flip, phase-flip, bit-phase-flip and depolarising noise channels to VRP circuits and

NoiseModel	Layers	NoiseParameter	AmplitudeDamping	BitFlip	BitPhaseFlip	DepolarisingNoise	PhaseFlip
6	1	0.05	-12.053	-13.768	-4.074	-4.949	-2.033
		0.1	-9.273	-9.577	-3.419	-2.437	-0.447
		0.15	-10.121	-9.661	-2.324	-0.750	-0.036
		0.2	-12.928	-9.614	-3.667	-0.608	0.049
		0.25	-12.491	-10.965	-3.638	-0.416	0.058
		0.3	-12.381	-10.383	-3.386	-0.261	0.059
		0.35	-11.519	-9.809	-3.696	-0.045	0.059
		0.4	-11.040	-9.881	-2.189	0.006	0.059
		0.45	-9.440	-10.531	-2.440	0.034	0.059
		0.5	-11.470	-11.999	-3.415	0.050	0.059
	2	0.05	-13.698	-4.262	-1.459	-2.377	-1.601
		0.1	-12.773	-6.576	-1.383	-0.748	-0.313
		0.15	-12.495	-6.282	-1.446	-0.305	-0.055
		0.2	-13.909	-5.872	-1.617	-0.052	0.058
		0.25	-13.171	-3.002	-1.267	0.029	0.058
		0.3	-12.834	-1.198	-1.296	0.055	0.059
		0.35	-13.162	-1.603	-1.296	0.058	0.059
		0.4	-12.760	-3.310	-1.184	0.059	0.059
		0.45	-13.789	-3.790	-1.064	0.059	0.059
		0.5	-12.986	-3.075	-1.511	0.059	0.059
12	1	0.05	-15.924	-2.332	-0.478	-1.167	-1.755
		0.1	-14.026	-1.392	-0.446	-0.396	-0.476
		0.15	-14.959	-3.239	-0.576	-0.031	-0.014
		0.2	-12.909	-1.634	-0.507	0.053	0.058
		0.25	-14.413	-2.651	-0.621	0.058	0.059
		0.3	-15.029	-0.910	-0.650	0.059	0.059
		0.35	-14.156	-1.864	-0.594	0.059	0.059
		0.4	-13.519	-1.784	-0.448	0.059	0.059
		0.45	-15.388	-1.621	-0.560	0.059	0.059
		0.5	-14.477	-0.488	-0.563	0.059	0.059
	2	0.05	-15.659	-0.969	-0.280	-0.681	-1.574
		0.1	-15.055	-1.494	-0.296	-0.052	-0.357
		0.15	-15.560	-0.213	-0.319	0.047	-0.022
		0.2	-14.661	-1.312	-0.335	0.059	0.059
		0.25	-14.771	-0.502	-0.322	0.059	0.059
		0.3	-16.147	-0.193	-0.246	0.059	0.059
		0.35	-13.468	-0.238	-0.301	0.059	0.059
		0.4	-13.916	0.012	-0.359	0.059	0.059
		0.45	-13.427	-0.886	-0.218	0.059	0.059
		0.5	-15.757	-0.074	-0.294	0.059	0.059
12	1	0.05	-42.626	-31.086	-1.855	-3.741	-1.056
		0.1	-42.157	-33.947	-1.448	-0.919	-0.514
		0.15	-38.465	-22.328	-2.387	-0.669	-0.660
		0.2	-37.787	-38.835	-2.260	-0.637	-0.581
		0.25	-46.766	-20.722	-1.696	-0.599	-0.699
		0.3	-41.555	-30.384	-2.556	-0.653	-0.567
		0.35	-37.722	-37.187	-2.454	-0.312	-0.444
		0.4	-38.388	-35.172	-1.951	-0.618	-0.548
		0.45	-40.835	-35.500	-1.909	-0.545	-0.482
		0.5	-47.219	-45.676	-2.387	-0.565	-0.577
	2	0.05	-47.215	-13.251	-0.240	-0.718	-0.658
		0.1	-43.464	-11.857	-0.166	-0.258	-0.410
		0.15	-40.368	-7.993	-0.223	-0.208	-0.383
		0.2	-45.283	-2.685	-0.178	-0.242	-0.178
		0.25	-48.947	-7.242	-0.229	-0.231	-0.363
		0.3	-36.999	-5.921	-0.250	-0.209	-0.192
		0.35	-44.922	-0.137	-0.213	-0.454	-0.255
		0.4	-43.944	-9.986	-0.232	-0.113	-0.313
		0.45	-46.463	-0.921	-0.189	-0.444	-0.274
		0.5	-43.890	-1.931	-0.200	-0.599	-0.211
3	0.05	-46.368	-1.086	-0.610	-0.713	-0.662	
	0.1	-40.817	-0.656	-0.638	-0.690	-0.520	
	0.15	-37.797	-0.649	-0.683	-0.709	-0.786	
	0.2	-39.519	-4.338	-0.657	-0.649	-0.626	
	0.25	-48.781	-3.428	-0.679	-0.658	-0.823	
	0.3	-40.945	-1.416	-0.568	-0.576	-0.736	
	0.35	-38.358	-3.859	-0.599	-0.646	-0.539	
	0.4	-42.179	-3.328	-0.647	-0.605	-0.539	
	0.45	-41.264	-0.603	-0.670	-0.700	-0.523	
	0.5	-44.605	-2.647	-0.672	-0.613	-0.593	
4	0.05	-46.110	-0.565	-0.530	-0.643	-0.533	
	0.1	-42.539	-1.276	-0.653	-0.628	-0.577	
	0.15	-42.971	-0.596	-0.638	-0.650	-0.611	
	0.2	-44.977	-0.560	-0.649	-0.676	-0.653	
	0.25	-39.561	-0.781	-0.582	-0.567	-0.680	
	0.3	-44.023	-0.624	-0.663	-0.651	-0.539	
	0.35	-40.907	-0.657	-0.634	-0.599	-0.606	
	0.4	-42.012	-2.570	-0.573	-0.594	-0.585	
	0.45	-43.650	-0.604	-0.598	-0.569	-0.681	
	0.5	-42.357	-0.608	-0.539	-0.571	-0.686	

TABLE I: VQE simulation of amplitude damping, bit-flip, phase-flip, bit-phase-flip and depolarizing channel for 6 and 12 qubits with 4 layers involving optimizer COBYLA, where energy costs are averaged over 10 simulations.

analyzed the effects. We have found that amplitude damping noise causes the least impact on the results of an optimized variational circuit. In contrast bit-phase-flip, depolarising and phase-flip noise channels had the maximum negative impact.

In most cases, the effects of noise are minimal at the first layer of the VRP circuits. While additional layers improve upon the results in the noiseless case, the opposite is true in the case of noise. Since some noise will always be present in quantum circuits, a practical finding of our results is that the COBYLA classical optimizers performs best for VQE circuits as compared to the other available optimizers.

The work we have presented in this paper provides an interesting avenue in evaluating the effect of noise on detailed gate-based simulations of hybrid quantum algorithms for real-world applications. Noise is considered to be the most problematic aspect of today's intermediate scale devices, and hence understanding the details of the effects of noise is critical in

NoiseModel	Layers	NoiseParameter	AmplitudeDamping	BitFlip	BitPhaseFlip	DepolarisingNoise	PhaseFlip
6	1	0.05	5.631	3.917	13.610	12.736	15.651
		0.1	8.412	8.107	14.265	15.247	17.238
		0.15	7.563	8.023	15.360	16.934	17.649
		0.2	4.757	8.070	14.017	17.076	17.734
		0.25	5.194	6.719	14.046	17.269	17.742
		0.3	5.303	6.801	14.299	17.423	17.744
		0.35	6.165	7.875	13.989	17.639	17.744
		0.4	6.644	7.803	15.495	17.690	17.744
		0.45	8.244	7.153	15.245	17.718	17.744
		0.5	6.215	5.686	14.270	17.734	17.744
		0.05	3.986	13.423	16.225	15.307	16.084
		0.1	4.911	11.108	16.301	16.936	17.371
		0.15	5.189	11.402	16.239	17.379	17.630
		0.2	3.775	11.813	16.067	17.632	17.742
		12	1	0.05	4.513	14.683	16.417
0.1	4.851			16.487	16.388	17.739	17.744
0.15	4.522			16.081	16.388	17.742	17.744
0.2	4.925			14.374	16.501	17.744	17.744
0.25	3.895			13.894	16.620	17.744	17.744
0.3	4.698			14.610	16.173	17.744	17.744
0.35	1.760			15.352	17.206	16.518	15.929
0.4	3.658			16.392	17.039	17.289	17.208
0.45	2.686			14.445	17.108	17.653	17.670
0.5	4.776			16.051	17.177	17.737	17.742
0.05	3.271			15.033	17.064	17.742	17.742
0.1	2.655			16.774	17.034	17.744	17.744
0.15	3.529			15.820	17.091	17.744	17.744
0.2	4.165			15.901	17.236	17.744	17.744
0.25	2.297			16.063	17.124	17.744	17.744
12	2	0.3	3.307	17.187	17.122	17.744	17.744
		0.35	2.025	16.715	17.404	17.003	16.111
		0.4	2.629	16.190	17.389	17.632	17.328
		0.45	2.124	17.472	17.365	17.732	17.662
		0.5	3.023	16.373	17.349	17.743	17.743
		0.05	2.914	17.182	17.362	17.744	17.744
		0.1	1.537	17.492	17.439	17.744	17.744
		0.15	4.076	17.447	17.383	17.744	17.744
		0.2	3.769	17.672	17.325	17.744	17.744
		0.25	4.257	16.798	17.466	17.744	17.744
		0.3	1.927	17.610	17.390	17.744	17.744
		0.35	23.058	34.599	63.829	61.943	64.628
		0.4	23.528	31.738	64.237	64.765	65.171
		0.45	27.220	43.356	63.298	65.015	65.025
		0.5	27.898	26.890	63.424	65.048	65.104
12	3	0.05	18.919	44.963	63.988	65.086	65.076
		0.1	24.129	35.301	63.129	65.031	65.118
		0.15	27.963	28.498	63.231	65.173	65.241
		0.2	27.297	30.513	63.733	65.067	65.136
		0.25	24.850	30.185	63.776	65.140	65.203
		0.3	18.465	20.008	63.298	65.120	65.107
		0.35	18.469	52.433	65.445	64.967	65.026
		0.4	22.220	53.827	65.518	65.429	65.275
		0.45	23.317	57.691	65.462	65.477	65.302
		0.5	20.402	62.999	65.507	65.443	65.507
		0.05	16.737	38.443	65.455	65.453	65.322
		0.1	28.686	59.764	65.435	65.475	65.493
		0.15	20.763	65.548	65.472	65.231	65.430
		0.2	21.740	55.698	65.453	65.572	65.372
		0.25	19.222	64.753	65.496	65.241	65.411
12	4	0.3	21.995	63.692	65.485	65.425	65.474
		0.35	19.317	64.599	65.074	64.972	65.023
		0.4	24.868	65.029	65.047	64.994	65.164
		0.45	27.888	65.035	65.002	64.976	64.899
		0.5	26.165	61.347	65.028	65.036	65.059
		0.05	16.904	62.256	65.006	65.026	64.862
		0.1	24.740	64.269	65.117	65.108	64.949
		0.15	27.327	62.096	65.085	65.038	65.156
		0.2	23.306	63.356	65.038	65.079	65.146
		0.25	24.421	65.082	65.014	64.985	65.162
		0.3	21.079	63.038	65.013	65.072	65.092
		0.35	19.575	65.120	65.155	65.042	65.152
		0.4	23.145	64.408	65.031	65.057	65.108
		0.45	22.713	65.088	65.047	65.034	65.074
		0.5	20.707	65.124	65.036	65.008	65.031
0.05	26.124	64.903	65.103	65.117	65.004		
0.1	21.662	65.061	65.022	65.033	65.145		
0.15	24.778	65.028	65.051	65.086	65.079		
0.2	23.672	63.115	65.112	65.090	65.100		
0.25	22.034	65.080	65.087	65.116	65.004		
0.3	23.328	65.076	65.145	65.114	64.998		

TABLE II: Table listing the amount of deviation from classical minimum for VQE simulation VRP using amplitude damping, bit-flip, phase-flip, bit-phase-flip and depolarizing channels for 6 and 12 qubits with 4 layers using COBYLA as optimizer, where deviation values are averaged over 10 simulations.

understanding how to make the most effective use of them. In this article, we have considered COBYLA yet there is still room for study for the other optimizers, such as SPSA. We also aim to test compare these results to circuits run on small quantum devices. It would also be interesting to consider larger VRP instances in physical devices which are beyond the ability to simulate classically. Future work is also needed to analyze more detailed noise models guided by the measured characteristics from the real NISQ devices that are proposed to solve problems such as VRP.

ACKNOWLEDGMENT

The authors are grateful for the IBM Quantum Experience platform and their team for developing the Qiskit platform and providing an open access to their simulators for running

quantum circuits and performing the experiments reported here [33].

REFERENCES

- [1] A. Montanaro, “Quantum algorithms: an overview,” *npj Quantum Information*, vol. 2, no. 1, p. 15023, Jan. 2016. [Online]. Available: <https://doi.org/10.1038/npjqi.2015.23>
- [2] S. Jordan, “https://quantumalgorithmzoo.org/.” [Online]. Available: <https://quantumalgorithmzoo.org/#ONML>
- [3] E. Farhi, J. Goldstone, and S. Gutmann, *A Quantum Approximate Optimization Algorithm*, Nov. 2014. [Online]. Available: <https://arxiv.org/abs/1411.4028v1>
- [4] E. Farhi, J. Goldstone, S. Gutmann, and M. Sipser, *Quantum Computation by Adiabatic Evolution*, Jan. 2000. [Online]. Available: <https://arxiv.org/abs/quant-ph/0001106v1>
- [5] L. K. Grover, *A fast quantum mechanical algorithm for database search*, May 1996. [Online]. Available: <https://arxiv.org/abs/quant-ph/9605043v3>
- [6] V. Dasari, M. S. Im, and L. Beshaj, *Solving machine learning optimization problems using quantum computers*, M. Blowers, R. D. Hall, and V. R. Dasari, Eds. Online Only, United States: SPIE, apr 2020. [Online]. Available: <https://www.spiedigitallibrary.org/conference-proceedings-of-spie/11419/2565038/Solving-machine-learning-optimization-problems-using-quantum-computers/10.1117/12.2565038.full>
- [7] E. National Academies of Sciences, “Chapter: 3 Quantum Algorithms and Applications,” in *Quantum Computing: Progress and Prospects (2019)*. [Online]. Available: <https://www.nap.edu/catalog/25196/quantum-computing-progress-and-prospects>
- [8] S. Harwood, C. Gambella, D. Trenev, A. Simonetto, D. Bernal, and D. Greenberg, “Formulating and Solving Routing Problems on Quantum Computers,” *IEEE Transactions on Quantum Engineering*, vol. 2, pp. 1–17, 2021. [Online]. Available: <https://ieeexplore.ieee.org/document/9314905>
- [9] K. Srinivasan, S. Satyajit, B. K. Behera, and P. K. Panigrahi, “Efficient quantum algorithm for solving travelling salesman problem: An ibm quantum experience,” May 2018. [Online]. Available: <https://arxiv.org/abs/1805.10928v1>
- [10] S. Feld, C. Roch, T. Gabor, C. Seidel, F. Neukart, I. Galter, W. Mauerer, and C. Linnhoff-Popien, *A Hybrid Solution Method for the Capacitated Vehicle Routing Problem Using a Quantum Annealer*, 2019, vol. 6. [Online]. Available: <https://www.frontiersin.org/article/10.3389/fict.2019.00013>
- [11] Utkarsh, B. K. Behera, and P. K. Panigrahi, *Solving Vehicle Routing Problem Using Quantum Approximate Optimization Algorithm*, Feb. 2020. [Online]. Available: <https://arxiv.org/abs/2002.01351v1>
- [12] C. Papalitsas, T. Andronikos, K. Giannakis, G. Theocharopoulos, and S. Fanarioti, “A QUBO Model for the Traveling Salesman Problem with Time Windows,” *Algorithms*, vol. 12, no. 11, 2019. [Online]. Available: <https://www.mdpi.com/1999-4893/12/11/224>
- [13] F. Glover, G. Kochenberger, M. Ma, and Y. Du, “Quantum Bridge Analytics II: QUBO-Plus, network optimization and combinatorial chaining for asset exchange,” *4OR*, vol. 18, no. 4, pp. 387–417, 2020, publisher: Springer. [Online]. Available: https://ideas.repec.org/a/spr/ajqoor/v18y2020i4d10.1007_s10288-020-00464-9.html
- [14] G. Kochenberger, J.-K. Hao, F. Glover, M. Lewis, Z. Lü, H. Wang, and Y. Wang, “The unconstrained binary quadratic programming problem: A survey,” *Journal of Combinatorial Optimization*, vol. 28, Jul. 2014. [Online]. Available: <https://link.springer.com/article/10.1007/s10878-014-9734-0>
- [15] H. Irie, G. Wongpaisarnsin, M. Terabe, A. Miki, and S. Taguchi, “Quantum Annealing of Vehicle Routing Problem with Time, State and Capacity,” in *Quantum Technology and Optimization Problems*, ser. Lecture Notes in Computer Science, S. Feld and C. Linnhoff-Popien, Eds. Cham: Springer International Publishing, 2019, pp. 145–156. [Online]. Available: https://link.springer.com/chapter/10.1007/978-3-030-14082-3_13
- [16] A. Crispin and A. Syriachas, “Quantum Annealing Algorithm for Vehicle Scheduling,” in *2013 IEEE International Conference on Systems, Man, and Cybernetics*, Oct. 2013, pp. 3523–3528, iSSN: 1062-922X. [Online]. Available: <https://ieeexplore.ieee.org/document/6722384>
- [17] F. E. Office, “Application of Digital Annealer for Faster Combinatorial Optimization,” *FUJITSU Sci. Tech. J.*, vol. 55, no. 2, p. 7, 2019. [Online]. Available: <https://www.fujitsu.com/global/documents/about/resources/publications/fstj/archives/vol55-2/paper12.pdf>

- [18] E. Campos, D. Rabinovich, V. Akshay, and J. Biamonte, "Training saturation in layerwise quantum approximate optimization," *Phys. Rev. A*, vol. 104, no. 3, p. L030401, Sep. 2021, publisher: American Physical Society. [Online]. Available: <https://link.aps.org/doi/10.1103/PhysRevA.104.L030401>
- [19] S. Wang, E. Fontana, M. Cerezo, K. Sharma, A. Sone, L. Cincio, and P. J. Coles, "Noise-induced barren plateaus in variational quantum algorithms," *Nat Commun*, vol. 12, no. 1, p. 6961, Nov. 2021, number: 1 Publisher: Nature Publishing Group. [Online]. Available: <https://www.nature.com/articles/s41467-021-27045-6>
- [20] J. Marshall, F. Wudarski, S. Hadfield, and T. Hogg, "Characterizing local noise in QAOA circuits," *IOP SciNotes*, vol. 1, no. 2, p. 025208, aug 2020. [Online]. Available: <https://doi.org/10.1088/2633-1357/abb0d7>
- [21] W. Lavrijsen, A. Tudor, J. Müller, C. Iancu, and W. de Jong, "Classical Optimizers for Noisy Intermediate-Scale Quantum Devices," in *2020 IEEE International Conference on Quantum Computing and Engineering (QCE)*, Oct. 2020, pp. 267–277. [Online]. Available: <https://arxiv.org/abs/2004.03004>
- [22] M. Cerezo, A. Arrasmith, R. Babbush, S. C. Benjamin, S. Endo, K. Fujii, J. R. McClean, K. Mitarai, X. Yuan, L. Cincio, and P. J. Coles, "Variational Quantum Algorithms," *Nat Rev Phys*, vol. 3, no. 9, pp. 625–644, Sep. 2021, arXiv: 2012.09265. [Online]. Available: <http://arxiv.org/abs/2012.09265>
- [23] T. Albash and D. A. Lidar, "Adiabatic quantum computation," *Rev. Mod. Phys.*, vol. 90, no. 1, p. 015002, Jan. 2018, publisher: American Physical Society. [Online]. Available: <https://link.aps.org/doi/10.1103/RevModPhys.90.015002>
- [24] E. K. Grant and T. S. Humble, "Adiabatic Quantum Computing and Quantum Annealing," jul 2020, iISBN: 9780190871994. [Online]. Available: <https://oxfordre.com/physics/view/10.1093/acrefore/9780190871994.001.0001/acrefore-9780190871994-e-32>
- [25] Y. Sun, J.-Y. Zhang, M. S. Byrd, and L.-A. Wu, "Adiabatic Quantum Simulation Using Trotterization," *arXiv:1805.11568 [quant-ph]*, Jun. 2018, arXiv: 1805.11568. [Online]. Available: <http://arxiv.org/abs/1805.11568>
- [26] L. Zhou, S.-T. Wang, S. Choi, H. Pichler, and M. D. Lukin, "Quantum Approximate Optimization Algorithm: Performance, Mechanism, and Implementation on Near-Term Devices," *Phys. Rev. X*, vol. 10, no. 2, p. 021067, Jun. 2020, publisher: American Physical Society. [Online]. Available: <https://link.aps.org/doi/10.1103/PhysRevX.10.021067>
- [27] S. P. Singh, *The Ising Model: Brief Introduction and Its Application*. IntechOpen, Feb. 2020, publication Title: Solid State Physics - Metastable, Spintronics Materials and Mechanics of Deformable Bodies - Recent Progress. [Online]. Available: <https://www.intechopen.com/chapters/71210>
- [28] S. G. BRUSH, "History of the lenz-ising model," *Rev. Mod. Phys.*, vol. 39, pp. 883–893, Oct 1967. [Online]. Available: <https://link.aps.org/doi/10.1103/RevModPhys.39.883>
- [29] A. Lucas, "Ising formulations of many NP problems," *Frontiers in Physics*, vol. 2, 2014. [Online]. Available: <https://www.frontiersin.org/article/10.3389/fphy.2014.00005>
- [30] A. Peruzzo, J. McClean, P. Shadbolt, M.-H. Yung, X.-Q. Zhou, P. J. Love, A. Aspuru-Guzik, and J. L. O'Brien, "A variational eigenvalue solver on a photonic quantum processor," *Nature Communications*, vol. 5, no. 1, p. 4213, Jul. 2014. [Online]. Available: <https://doi.org/10.1038/ncomms5213>
- [31] P. Date, R. Patton, C. Schuman, and T. Potok, "Efficiently embedding QUBO problems on adiabatic quantum computers," *Quantum Information Processing*, vol. 18, no. 4, p. 117, Mar. 2019. [Online]. Available: <https://doi.org/10.1007/s11128-019-2236-3>
- [32] G. G. Guerreschi, "Solving Quadratic Unconstrained Binary Optimization with divide-and-conquer and quantum algorithms," *arXiv:2101.07813 [quant-ph]*, Jan. 2021, arXiv: 2101.07813. [Online]. Available: <http://arxiv.org/abs/2101.07813>
- [33] M. S. A. *et al.*, "Qiskit: An open-source framework for quantum computing," 2021. [Online]. Available: <https://github.com/Qiskit/qiskit/tree/0.25.0>
- [34] S. Ahadpour, F. Mirmasoudi, S. Ahadpour, and F. Mirmasoudi, "The role of noisy channels in quantum teleportation," *Revista mexicana de física*, vol. 66, no. 3, pp. 378–387, Jun. 2020, publisher: Sociedad Mexicana de Física. [Online]. Available: http://www.scielo.org.mx/scielo.php?script=sci_abstract&pid=S0035-001X2020000300378&lng=es&nrm=iso&tlng=en
- [35] R.-G. Zhou, Y.-N. Zhang, R. Xu, C. Qian, and I. Hou, "Asymmetric Bidirectional Controlled Teleportation by Using Nine-Qubit Entangled State in Noisy Environment," *IEEE Access*, vol. 7, pp. 75 247–75 264, 2019. [Online]. Available: <https://ieeexplore.ieee.org/document/8726306>